Surface Review and Letters, Vol. 29, No. 1 (2022) 2250008 (11 pages)

DOI: 10.1142/S0218625X22500081

World Scientific
www.worldscientific.com

EVALUATION OF MATERIAL REMOVAL RATE AND SURFACE ROUGHNESS IN WIRE ELECTRO-DISCHARGE MACHINING OF 10-WT.% ZrO_2-REINFORCED AL ALLOY COMPOSITE

A. KARTHIKEYAN*,§, S. V. ALAGARSAMY†,¶ and C. ILAIYA PERUMAL‡,‖

*Department of Mechanical Engineering,
University VOC College of Engineering,
Anna University Thoothukudi Campus,
Thoothukudi 628008, Tamil Nadu, India

†Department of Mechanical Engineering,
Mahath Amma Institute of Engineering & Technology,
Pudukkottai 622101, Tamil Nadu, India

‡Department of Mechanical Engineering,
Alagappa Chettiar Government College of
Engineering and Technology,
Karaikudi, Sivagangai 630004, Tamil Nadu, India
§karthikeyan.me@gmail.com
¶s.alagarsamy88@gmail.com
‖ipdesign2012@gmail.com

Received 1 April 2021
Revised 2 September 2021
Accepted 25 September 2021
Published 8 November 2021

In this study, we optimize the wire electro-discharge machining (WEDM) parameters in zirconia (ZrO_2) ceramic particulates-filled Al7075 alloy composite by using the Taguchi-combined Technique for Order Preference by Similarity to Ideal Solution (TOPSIS) method. The Al7075 alloy composite was synthesized via the stir casting route by the addition of 10 wt.% of ZrO_2 particulates. Scanning electron microscopy (SEM) was used to analyze the microstructure of fabricated composite. Experimental work was executed as per the $L_9(3^3)$ orthogonal array design by considering three input machining parameters like pulse current (I_p), pulse on-time (T_{on}) and pulse off-time (T_{off}), respectively. The material removal rate (MRR) and surface roughness (SR) were chosen as the output responses for machining of the developed composite. The signal-to-noise (S/N) ratio was employed to determine the optimum levels of machining parameters for the output responses. Moreover, analysis of variance (ANOVA) was used to find the significant contribution of parameters. The main effect plot explored that I_p of 25 A, T_{on} of 115 μs and T_{off} of 60 μs were identified as the optimum levels of machining parameters which provide the maximum MRR (0.36757 g/min) and minimum SR (3.826 μm) for the proposed composite during the WEDM process. ANOVA results revealed that I_p was the most dominant factor regarding MRR and SR followed by T_{on} with contributions of 74.05% and 14.48%, respectively.

Keywords: Al7075 alloy; ZrO_2; stir casting; composite; WEDM parameters; Taguchi method; TOPSIS method; ANOVA.

§Corresponding author.

1. Introduction

Nowadays, the scope for new materials in the current innovative production industries has resulted in the potential growth of novel materials that have unique characteristics for practical use. The metal matrix composites (MMCs) are gaining more significance owing to their enhanced mechanical properties than the unreinforced alloys for assorted specific applications in aerospace, automotive and nuclear industries.[1,2] Aluminum matrix composites (AMCs) are most favorable due to their unique specifications such as high strength, good elastic modulus, high hardness and better wear resistance.[3] Generally, AMCs are developed through various techniques like powder metallurgy, stir casting, compo-casting, infiltration and spray deposition method. Among them, stir casting method is the most opted route for fabrication of AMCs due to its benefits like simplicity, cost effectiveness, mass production ability and achievement of uniform particles distribution by stirring action.[4] The inclusion of hard ceramic particles as the reinforcement made these composites difficult to machine using the conventional metal removing process. As a result, those composites have limited applications like in the small production of only specific components. Alternatively, the unconventional machining processes have prolonged their significance for the machining of MMCs.[5] However, the unconventional machining processes involve more economic equipment and intricate shapes to be machined in the components with high tolerance and precision.[6,7] Among the various unconventional machining processes, wire electro-discharge machining (WEDM) process has been a universally well-known efficient and economical method used to machine complicate shapes in the materials.[8,9] During the WEDM process, the metal is eroded by producing a sequence of electric sparks between the electrode and workpiece.[10] Hence, the WEDM process is suitable for machining of MMCs for developing complex geometries with a better dimensional accuracy. Discharge current, voltage, pulse duration, wire tension, wire speed and dielectric fluid are the influencing variables in the WEDM process, whereas the metal removal rate (MRR), surface roughness (SR) and kerf width (K) are selected as the output variables for measuring the performance of machinability.[11,12] To gain the knowledge on machinability of MMCs, several researchers investigated the effect of various input parameters on the responses during the WEDM process.[13–21] Liu *et al.*[13] described the WEDM of Al_2O_3 particulates-reinforced AA6061 composites by considering various input parameters, namely current, pulse on-time (T_{on}) and pulse off-time (T_{off}). They reported that applied current was the predominant factor for enhancing the MRR. Rao[14] optimized the WEDM process parameters based on multiple quality characteristics for the machining of Al7075/SiC MMCs. They revealed that particle size and pulse on-time are the most impacting parameters, followed by wire tension. Mahapatra and Patnaik[15] attempted to determine the optimum machining parameters, viz. current, pulse duration, wire speed, wire tension and dielectric flow, for MRR and SR using the Taguchi method. They concluded that higher MRR and lower SR were achieved by moderate setting of the current and duration of pulse. Bobbili *et al.*[16] studied the WEDM process of AA7075 by using brass electrode and found that the maximum current and higher pulse on-time enhanced the craters on the cutting surface, thus resulting in an increased SR. Ramabalan *et al.*[17] presented the effects of reinforcement content on MRR during the WEDM process of composites of AA7075 filled with TiB_2 particulates. They concluded that the minimum MRR was obtained by the TiB_2-reinforced AA7075 composites due to the addition of hard reinforcements that improved the hardness. Udaya Prakash *et al.*[18] studied the WEDM parameters for the machining of hybrid composite using Taguchi technique and reported that the voltage is the most impacting factor for enhancing the MRR. From the analysis of variance (ANOVA) results, they found that gap voltage and pulse on-time are the most impacting parameters on the responses. Sreeraj *et al.*[19] employed the WEDM process for AA6351/rutile composite by considering the effect of various parameters, namely, current, voltage and wire speed, on SR and kerf width. They reported that current was the significant factor concerning SR followed by voltage and wire feed rate, respectively. Lenin *et al.*[20] studied the WEDM parameters of Al-LM25/fly ash/B_4C hybrid composites fabricated through stir casting technique. They reported that the gap voltage and pulse on-time were the most decisive factors for SR and volume removal rate (VRR). Kumar *et al.*[21] investigated the WEDM behavior of hybrid Al6061 composites reinforced with

silicon carbide, graphite and iron oxide, respectively. They observed that an increase in pulse current and pulse on-time increases the MRR due to rapid and repetitive spark developed during the machining process.

In this study, we describe the impact of WEDM machining parameters viz. pulse current (I_p), T_{on} and T_{off} on the MRR and SR during the machining of 10-wt.% zirconia (ZrO_2)-reinforced Al7075 alloy composite fabricated by the stir casting method. Taguchi-combined Technique for Order Preference by Similarity to Ideal Solution (TOPSIS) method was applied to find out the optimal levels of machining parameters for the multiple-objective responses. At last, ANOVA was carried out to determine the significance of parameters for the responses.

2. Experimental Details

2.1. *Fabrication of composite*

In this study, Al7075 alloy was considered as a matrix element which was procured from the Coimbatore metal mart and ZrO_2 was selected as the reinforcement elements which were purchased from Loba Chemie, Mumbai. The elements composition (in wt.%) of Al7075 alloy is as follows: Zn: 5.4, Mg: 2.42, Cu: 1.42, Fe: 0.42, Cr: 0.21, Si: 0.13, Mn: 0.12, Ti: 0.11 and Al: remaining. The reason for selecting Al7075 alloy is its uniqueness of properties like high strength-to-weight ratio, better thermal properties and natural aging characteristics which have more importance in the aerospace and automotive industries. The basis for choosing ZrO_2 is that the particles acquired good hardness as well as better corrosion and wear resistance. The composite was produced through the stir casting route. Initially, 0.9 kg of Al7075 alloy rod was kept in a crucible made of graphite and it was melted at 850°C using electrical furnace.[22] To improve the wettability, 0.1 kg (10 wt.%) of ZrO_2 particles were preheated at a temperature of 200°C using muffle furnace. The preheated ZrO_2 (10 wt.%) reinforcement particles were introduced manually into the molten metal of Al alloy. After that, the stirrer was used to stir the composite slurry at 280 rpm for 10 min.[23] Finally, the composite mixture was transferred into a metallic mold and solidified at room temperature. The microstructure of the fabricated composite was observed by scanning electron microscopy (SEM; VEGA3 TESCAN, Czech Republic). Figure 1 displays the SEM image of the developed composite and

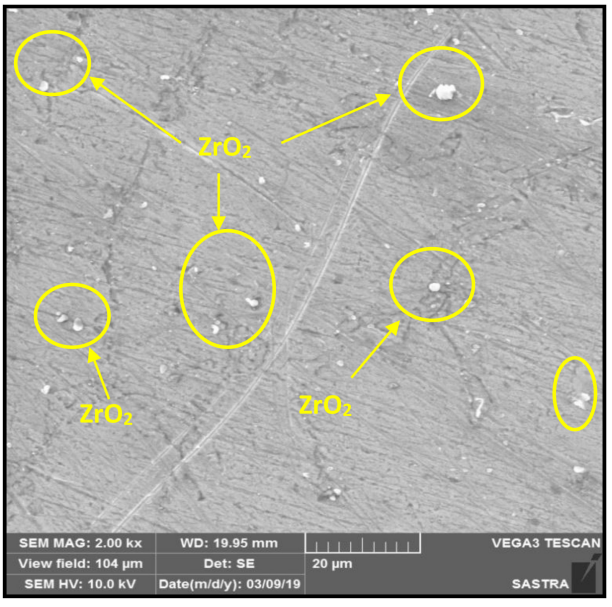

Fig. 1. SEM image of 10-wt.% ZrO_2–Al7075 alloy composite.

the presence of ZrO_2 particulates over the matrix alloy is evident in the figure.

2.2. *Design of experiments*

From the earlier researches, it was found that a set of process parameters strongly influenced the WEDM performance including MRR and SR. Therefore, three process parameters, namely, I_p, T_{on} and T_{off}, were suggested as the input machining parameters. The preferred machining factors with their levels are presented in Table 1. As per the selection of the parameters and their levels, L_9 (3^3) orthogonal array was formulated for the experimental trials.

2.3. *WEDM process of composite*

The experimental work was carried out on an ECO-CUT CNC WEDM machine displayed in Fig. 2. A brass wire of 0.25-mm diameter was used as an

Table 1. Machining parameters and their levels.

			Levels		
Notation	Machining parameter	Unit	1	2	3
I_p	Pulse current	A	25	50	75
T_{on}	Pulse on-time	µs	115	130	145
T_{off}	Pulse off-time	µs	20	40	60

Fig. 2. ECOCUT CNC WEDM machine.

Fig. 3. Machined Al7075 alloy–10-wt.% ZrO_2 composite.

electrode and deionized water was used as a dielectric fluid. The brass wire was typically alloyed with copper (63–65%) and zinc (35–37%). Earlier studies stated that the addition of zinc enhances the cutting performance and speed compared to copper wire.[24] During experimental trials, square specimens of dimensions 10 mm × 10 mm were machined with a length of 30 mm. Figure 3 illustrates the photographic view of machined composite specimens. An L_9 (3^3) array was formulated as a work plan layout of the WEDM process.

During the research, the performance of WEDM is evaluated by two important responses, i.e. MRR and SR. A total number of nine trials were performed according to the formulated work layout of Table 2. MRR was estimated by the ratio of weights before and after machining under an elapsed time. The following equation was applied to calculate the MRR[25]:

$$\text{MRR} = \frac{W_i - W_f}{T_m}\ \text{g/min}, \tag{1}$$

where W_i and W_f are the initial and final weights of the workpiece (g), and T_m is the machining time (min).

Table 2. L_9 orthogonal array of input parameters and output responses.

Exp. no.	Pulse current, I_p (A)	Pulse on-time, T_{on} (μs)	Pulse off-time, T_{off} (μs)	MRR (g/min)	SR (μm)
1	25	115	20	0.28460	2.853
2	25	130	40	0.32542	3.641
3	25	145	60	0.36757	3.826
4	50	115	40	0.26420	3.582
5	50	130	60	0.31286	4.358
6	50	145	20	0.34262	4.657
7	75	115	60	0.24139	3.157
8	75	130	20	0.30453	5.214
9	75	145	40	0.32780	5.014

The SR value was estimated on each machined surface of the composite at different places by using Mitutoyo Talysurf SJ-210 surface roughness tester. The average SR value was used to perform the statistical analysis. The experimental parameters and their corresponding output responses are provided in Table 2.

3. Methodologies and Implementations

3.1. *Taguchi method*

Signal-to-noise (S/N) ratio was used to obtain the optimum levels of machining parameters for the desired output results in Taguchi analysis. Typically, three types of responses have been feasible to evaluate the S/N ratio such as larger-the-better, nominal-the-better and smaller-the-better.[26] In this research, we are in need of higher MRR with lower SR. Therefore, larger-the-better was preferred for MRR and smaller-the-better was selected for SR. The following equations are used to compute the S/N ratios of output responses:

$$\text{S/N ratio} = -10\log_{10}(1/n)\sum_{k=1}^{n}\frac{1}{Y_{ij}^2}, \tag{2}$$

$$\text{S/N ratio} = -10\log_{10}(1/n)\sum_{k=1}^{n}Y_{ij}^2, \tag{3}$$

where n is the number of factors, Y_{ij} denotes the response, where $i = 1, 2, 3, \ldots, n$ and $j = 1, 2, 3, \ldots, k$. The estimated responses and their calculated S/N ratios are given in Table 3. ANOVA technique is employed to observe the effects of factors on the responses under investigation.[27] Here, ANOVA was

Table 3. Output responses and their S/N ratios.

	Output responses		S/N ratios	
Exp. no.	MRR (g/min)	SR (μm)	MRR (dB)	SR (dB)
1	0.28460	2.853	−10.9153	−9.10604
2	0.32542	3.641	−9.75110	−11.2244
3	0.36757	3.826	−8.69320	−11.6549
4	0.26420	3.582	−11.5613	−11.0825
5	0.31286	4.358	−10.0930	−12.7857
6	0.34262	4.657	−9.30370	−13.3621
7	0.24139	3.157	−12.3456	−9.98549
8	0.30453	5.214	−10.3274	−14.3434
9	0.32780	5.014	−9.68780	−14.0037

applied to determine the importance of parameters such as I_p, T_{on} and T_{off} for MRR and SR and also to estimate the percentage contributions of those parameters.

3.2. *TOPSIS method*

TOPSIS approach was introduced by Hwang and Yoon in 1995, which is extensively employed to find out the optimum parameters for multiple response characteristics.[28] The main objective of this approach is that it is applied to determine the best alternative from the ideal solution. The maximization of benefit criterion and minimization of cost criterion are obtained by positive ideal solution. The minimization of benefit criterion and maximization of cost criterion are obtained by negative ideal solution. The optimum alternative is closer to the positive ideal solution and farthest from the negative ideal solution. The following steps are to be followed under the TOPSIS method:

Step 1. The first step is to determine the normalized decision matrix. The normalized value r_{ij} is evaluated by using

$$r_{ij} = x_{ij}\sqrt{\sum_{i-1}^{m} x_{ij}^2},$$

$$i = 1, 2, \ldots, m \quad \text{and} \quad j = 1, 2, \ldots, n. \quad (4)$$

Step 2. Here, the weighted normalized decision matrix is computed. It was obtained by using

$$v_{ij} = r_{ij} \times w_j, i = 1, 2, \ldots, m \text{ and } j = 1, 2, \ldots, n, \quad (5)$$

where w_j is the weight of the jth criterion and $\sum_{j=1}^{n} w_j = 0.5$. Table 4 shows the calculated normalized matrix and the weighted normalized matrix.

Table 4. Normalized matrix and weighted normalized matrix.

	Normalized decision matrix (r_{ij})		Weighted normalized decision matrix (v_{ij})	
Exp. no.	MRR	SR	MRR	SR
1	0.30591	0.231518	0.152955	0.115759
2	0.349786	0.295464	0.174893	0.147732
3	0.395092	0.310476	0.197546	0.155238
4	0.283982	0.290676	0.141991	0.145338
5	0.336286	0.353648	0.168143	0.176824
6	0.368274	0.377911	0.184137	0.188956
7	0.259464	0.256188	0.129732	0.128094
8	0.327332	0.423111	0.163666	0.211556
9	0.352344	0.406881	0.176172	0.203441

Step 3. In this step, the positive (A^*) and negative (A^-) ideal solutions are determined as follows:

$$A^* = \{(\max_i v_{ij} | j \in C_b), (\min_i v_{ij} | j \in C_c)\} = \{v_j^* | j = 1, 2, \ldots, m\}, \quad (6)$$

$$A^- = \{(\min_i v_{ij} | j \in C_b), (\max_i v_{ij} | j \in C_c)\} = \{v_j^- | j = 1, 2, \ldots, m\}, \quad (7)$$

where max v_{ij} denotes the maximum value of normalized weight matrix and min v_{ij} is the minimum value of normalized weight matrix. Table 5 presents the obtained positive and negative ideal solutions.

Step 4. To find the separation measures individually, alternative positive and negative ideal solutions are computed by using the following equations:

$$S_i^* = \sqrt{\sum_{j=1}^{m} (v_{ij} - v_j^*)^2}, \quad j = 1, 2, \ldots, m, \quad (8)$$

Table 5. Positive and negative ideal solutions.

Response	MRR	SR
A^*	0.197546	0.115759
A^-	0.129732	0.211556

$$S_i^- = \sqrt{\sum_{j=1}^{m} (v_{ij} - v_j^-)^2}, \quad j = 1, 2, \ldots, m. \tag{9}$$

Step 5. Finally, we need to estimate the relative closeness (RC) value from the separation measures of the ideal solutions. The relative closeness is obtained from

$$\mathrm{RC}_i^* = \frac{S_i^-}{S_i^* + S_i^-}, \quad i = 1, 2, \ldots, m. \tag{10}$$

Table 6 shows the separation measures of the ideal solutions and the relative closeness values with their ranks.

Figure 4 displays the rank plot for relative closeness value versus the experiment number. According to Fig. 4, the order of relative closeness values is 2–3–1–5–7–6–4–9–8. It was clearly found that experiment number 3 has obtained the highest relative closeness which recommends the combination of machining parameters nearer to their optimum levels.

Table 6. Separation measures and relative closeness values with their ranks.

	Separation measures		Relative closeness	
Exp. no.	S_i^*	S_i^-	(RC_i^*)	Rank
1	0.044591	0.098571	0.688528	2
2	0.039184	0.078186	0.666147	3
3	0.039479	0.088150	0.690673	1
4	0.062939	0.067343	0.516904	5
5	0.067775	0.051785	0.433131	7
6	0.074415	0.058912	0.441864	6
7	0.068927	0.083462	0.547693	4
8	0.101611	0.033934	0.250352	9
9	0.090249	0.047144	0.343131	8

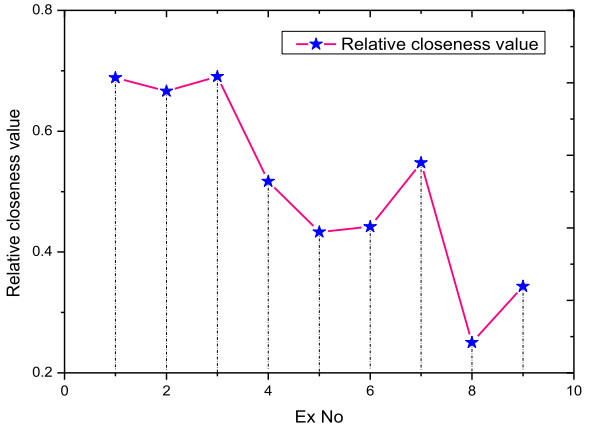

Fig. 4. Rank plot for relative closeness.

4. Results and Discussion

4.1. *Analysis of machining parameters for MRR*

Table 7 depicts the mean S/N ratio of MRR. In the table, the effects of parameters on the response are observed by the delta values. The largest delta value is represented as rank 1. The mean value of the S/N ratio for MRR is −10.2976 dB. From Table 7, it can be noticed that pulse on-time was the most significant factor for MRR, followed by pulse current. MRR increases due to increase in current and pulse on-time. The reason could be that an increase in I_p and T_{on} creates longer spark duration which develops more heat on the workpiece, thus improving the MRR.

Figure 5 displays the main effect plot for the mean S/N ratio of MRR with respect to machining parameters at each level. From Fig. 5, it can be understood that the optimum levels of machining

Table 7. Response table for the mean S/N ratio of MRR.

	Levels				
Parameter	1	2	3	Delta	Rank
I_p	−9.787	−10.319	−10.787	1	2
T_{on}	−11.607	−10.057	−9.228	2.379	1
T_{off}	−10.182	−10.333	−10.377	0.195	3
Mean S/N ratio of MRR = −10.2976					

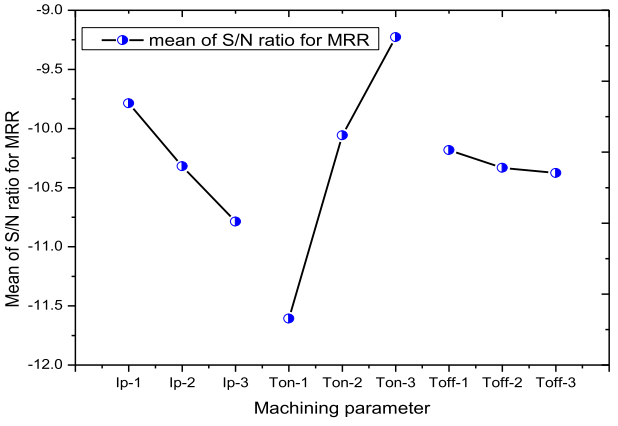

Fig. 5. Main effect plot for the mean S/N ratio of MRR.

Table 8. Analysis of variance for MRR.

Source	DoFs	Seq. SS	Adj. SS	Adj. MS	F-ratio	p (%)
I_p	2	0.0018061	0.0018061	0.0009030	14.85	14.58
T_{on}	2	0.0104174	0.0104174	0.0052087	85.66	84.13
T_{off}	2	0.0000359	0.0000359	0.0000180	0.30	0.29
—Error	2	0.0001216	0.0001216	0.0000608	—	0.98
Total	8	0.0123811	—	—	—	—

$S = 0.00779768$; $R^2 = 99.02\%$; and adj.-$R^2 = 96.07\%$.

parameters for obtaining the maximum MRR are: I_p at level 1 (25 A), T_{on} at level 3 (145 μs) and T_{off} at level 1 (20 μs), respectively.

ANOVA result for MRR is shown in Table 8. It can be explored that the percentage of contribution of each parameter is estimated by the ratio of sum of squares (SS) to the total sum of squares (TSS). According to the table, the F-ratios of $T_{on}(F = 85.66)$ and I_p $(F = 14.85)$ were greater than that of T_{off}, which ensures that those factors have a statistical influence on MRR. It was also found that T_{on} and I_p are the most dominant factors regarding MRR with contributions of 84.13% and 14.58%, respectively. T_{off} was a less significant factor with a contribution of 0.29% only. Similar observations were reported by Alduroobi *et al.*[29] during the WEDM process of AISI 1045 steel. The R^2 and adj.-R^2 values of 99.02% and 96.07% are very close to each other, which indicated that the design was able to predict with high accuracy. Figure 6 shows the probability graph for MRR; it revealed that the response values are placed on a straight line, which means that the residuals are uniformly scattered for the proposed model.

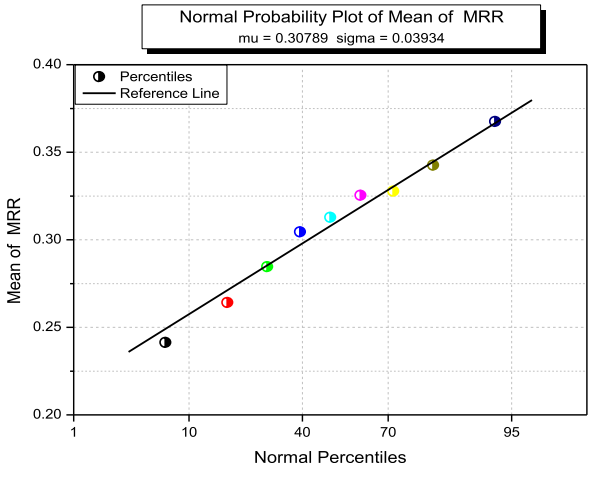

Fig. 6. Probability plot for MRR.

4.2. *Analysis of machining parameters for SR*

Table 9 depicted the mean S/N ratio for SR. In the table, a higher delta value is represented as rank 1, which indicates the most significant factor. The mean S/N ratio for SR is −11.9498 dB. From Table 9, it is revealed that pulse on-time is the chief control factor for SR, followed by pulse current. The SR value of machined composite mainly depends on the applied current and pulse on-time during machining. The increase in I_p and pulse duration increases the SR due to more spark energy producing larger craters over the machined surface of the composite.[19]

Figure 7 illustrates the main effect plot for the mean S/N ratio of SR with respect to WEDM machining parameters. From the figure, it is observed that the optimum levels of machining parameters for minimum SR are as follows: I_p at level 1 (25 A), T_{on} at level 1 (115 μs) and T_{off} at level 3 (60 μs), respectively.

ANOVA result for SR is presented in Table 10. From the table, the F-ratios of pulse on-time $(F = 13.46)$ and pulse current $(F = 7.20)$ were

Table 9. Response table for the mean S/N ratio of SR.

	Levels				
Parameter	1	2	3	Delta	Rank
I_p	−10.66	−12.41	−12.78	2.12	2
T_{on}	−10.06	−12.78	−13.01	2.95	1
T_{off}	−12.27	−12.10	−11.48	0.80	3

Mean S/N ratio of SR = −11.9498

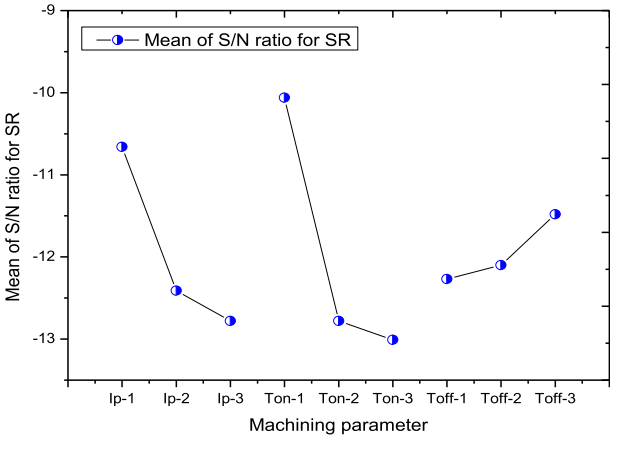

Fig. 7. Main effect plot for the mean S/N ratio of SR.

Table 10. Analysis of variance for SR.

Source	DoFs	Seq. SS	Adj. SS	Adj. MS	F-ratio	p (%)
I_p	2	1.6889	1.6889	0.8444	7.20	31.20
T_{on}	2	3.1601	3.1601	1.5801	13.46	58.32
T_{off}	2	0.3281	0.3281	0.1640	1.40	6.06
Error	2	0.2347	0.2347	0.1174	—	4.33
Total	8	5.4118	—	—	—	—

$S = 0.342572$; $R^2 = 95.66\%$; and adj.-$R^2 = 82.65\%$.

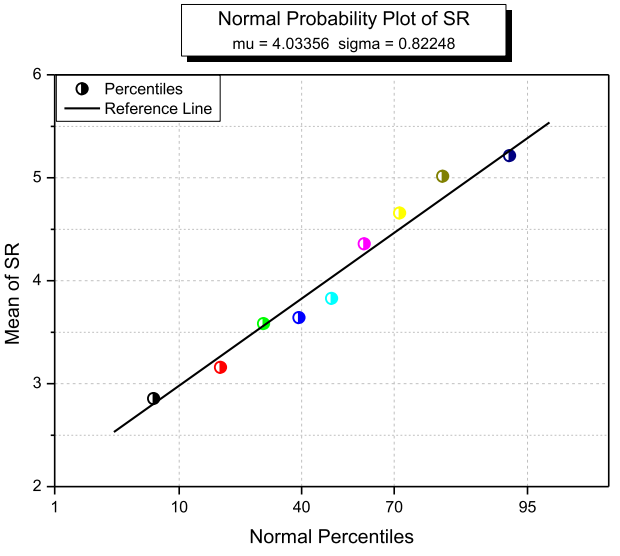

Fig. 8. Probability plot for SR.

greater than that of pulse off-time, which ensures that those factors are statistically significant for SR. It was also revealed that T_{on} and I_p are the most impacting parameters for SR with the contributions of 58.32% and 31.20%, respectively. Similar results were reported by Rao and Krishna[30] while machining the Al7075/SiC_p metal matrix composites. The pulse off-time was a less significant factor with a contribution of 6.06% only. The R^2 and adj.-R^2 values of 95.66% and 82.65% are very near to each other, which indicates that the model was able to predict with high accuracy. The probability plot for SR is displayed in Fig. 8; it shows that the response values are located on a straight line, which represents that the residuals are evenly scattered for the planned model.

4.3. *Analysis of machining parameters for relative closeness*

Table 11 represents the mean relative closeness at individual level of the parameters and the average

Table 11. Response table for the mean relative closeness.

	Levels				
Parameter	1	2	3	Delta	Rank
I_p	0.6818	0.4640	0.3804	0.3014	1
T_{on}	0.5844	0.4499	0.4919	0.1345	2
T_{off}	0.4602	0.5087	0.5572	0.0969	3

Mean relative closeness value = 0.508714

relative closeness. From the table, the average value of mean relative closeness is 0.508714. The maximum delta value of pulse current indicates that it is the most significant parameter for multiple responses, followed by pulse on-time. The reason behind is that an increase in current enhances the development of heat generation which leads to an increase in MRR and SR being achieved.

Figure 9 exhibits the main effect plot for the mean value of relative closeness with respect to machining parameters. From Fig. 9, it can be clearly explored that the optimum combination of machining parameters for higher MRR with lower SR is attained as follows: I_p at level 1 (25 A), T_{on} at level 1 (115 μs) and T_{off} at level 3 (60 μs), respectively.

ANOVA results for relative closeness are depicted in Table 12. From the table, the F-ratios of I_p ($F = 17.29$) and T_{on} ($F = 3.38$) were larger than that of T_{off} ($F = 1.68$), which ensured that those factors statistically influenced multiple responses. It has also been confirmed that I_p was the strongest affecting parameter with a contribution of 74.05%, followed by T_{on} and T_{off} with the contributions of 14.48% and 7.18%, respectively. The error contribution was only

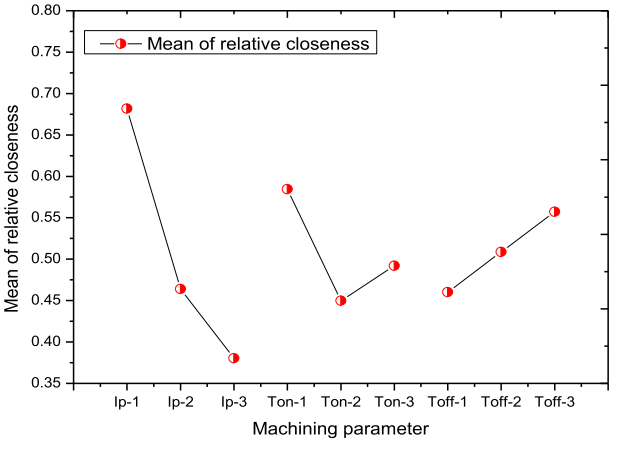

Fig. 9. Main effect plot for the mean relative closeness.

Table 12. Analysis of variance for relative closeness.

Source	DoFs	Seq. SS	Adj. SS	Adj. MS	F-ratio	p (%)
I_p	2	0.145265	0.145265	0.072633	17.29	74.05
T_{on}	2	0.028409	0.028409	0.014204	3.38	14.48
T_{off}	2	0.014090	0.014090	0.007045	1.68	7.18
Error	2	0.008401	0.008401	0.004201	—	4.28
Total	8	0.196164	—	—	—	—

$S = 0.0648116$; $R^2 = 95.72\%$; and adj.-$R^2 = 82.87\%$.

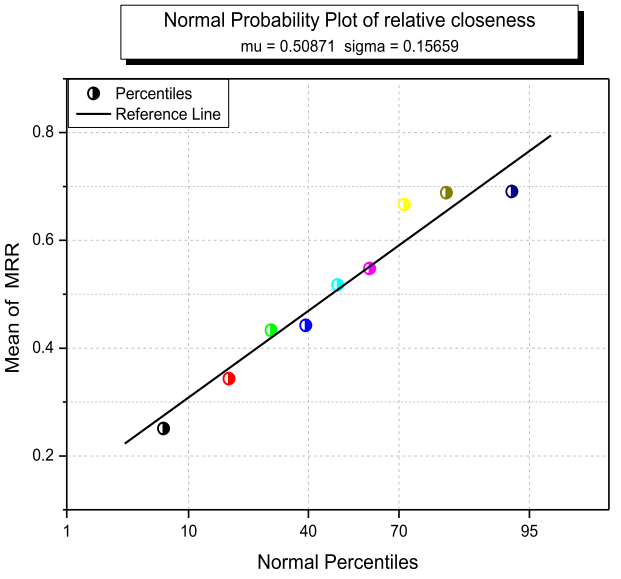

Fig. 10. Probability plot for relative closeness.

4.28%. The R^2 and adj.-R^2 values of 95.72% and 82.87% are very close to each other which shows that the model has predicted with high accuracy. Figure 10 depicts the probability plot for relative closeness; it reveals that the responses are to be found within a limit, which ensures that the data are regularly disseminated for the created model.

4.4. *Contour plot analysis*

Figures 11(a)–11(c) display the contour graphs for relative closeness for the WEDM process parameters. In Fig. 11(a), the effect of I_p and T_{on} on relative closeness is demonstrated. It was found that the relative closeness value regularly decreases with increase in T_{on} at a low setting of I_p. However, the maximum relative closeness value of 0.66 is obtained at the initial current of 25 A and a pulse on-time of 145 μs. When the pulse on-time started to increase, the

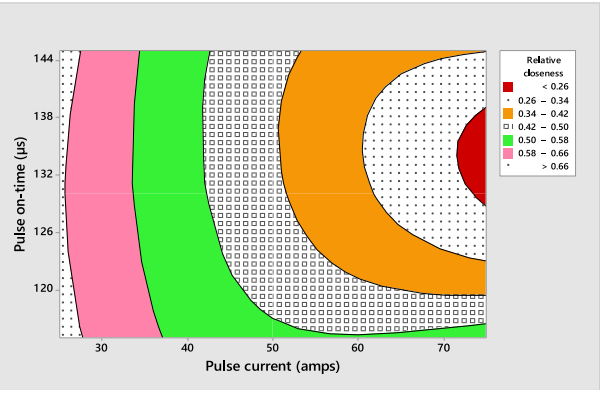

(a)

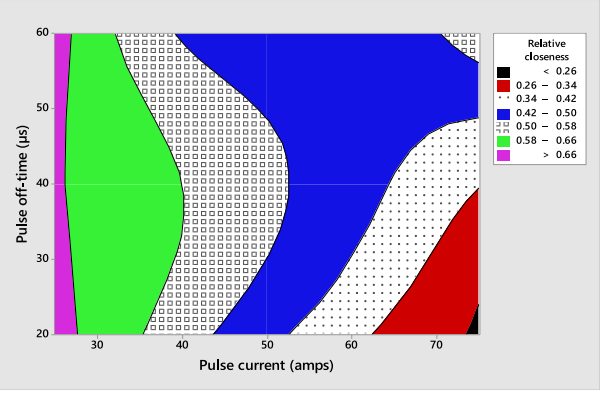

(b)

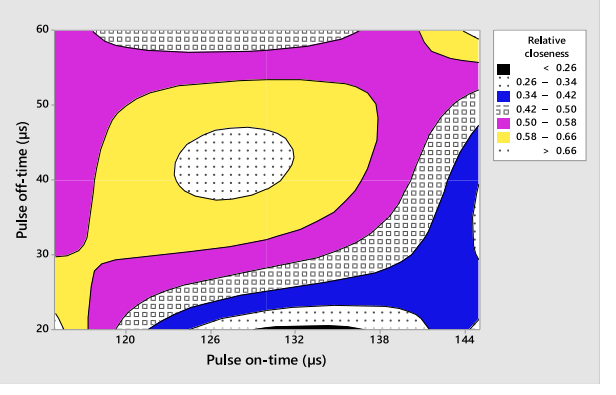

(c)

Fig. 11. Contour plots for relative closeness: (a) I_p versus T_{on}, (b) I_p versus T_{off} and (c) T_{on} versus T_{off}.

relative closeness improved gradually during machining. It was also understood that the minimum relative closeness of 0.26 was attained at the middle level of pulse on-time of 130 μs and at higher level of current of 75 A.

Figure 11(b) reveals the effect of I_p and T_{off} on relative closeness. From the figure, it can be explored that the maximum relative closeness value of 0.66 is achieved by the initial level of I_p (25 A) at any level of T_{off}. The reason is that pulse off-time is a less significant factor than the others; hence it did not affect the responses. The minimum relative closeness value of 0.26 was achieved by the high-level current of 75 A and middle-level pulse off-time of 30 μs.

Figure 11(c) shows the responses of relative closeness value with respect to T_{on} and T_{off}. It was found that the maximum value of relative closeness of 0.66 was achieved at the moderate levels of pulse on-time of 130 μs and pulse off-time of 40 μs. However, the middle level of pulse on-time of 130 μs gradually decreases the relative closeness value due to significant effects of parameter conditions on the responses. By comparing T_{on} and T_{off} with respect to response characteristics, T_{on} was the most dominant parameter as well as T_{off} has an insignificant effect on the responses.

5. Conclusions

The following are the conclusions of this study:

- In this research work, the composite of Al7075 alloy reinforced with 10-wt.% ZrO_2 particles was effectively synthesized via stir casting route and the WEDM process was studied.
- The SEM micrograph reveals that the ZrO_2 particulates are uniformly distributed in the Al7075 alloy matrix.
- Taguchi-combined TOPSIS method was efficiently employed to select the optimum levels of WEDM parameters such as I_p, T_{on} and T_{off} for MRR and SR.
- From the S/N ratio analysis, the higher MRR is obtained at: I_p: 25 A, T_{on}: 145 μs and T_{off}: 20 μs. Similarly, the lower SR is attained at: I_p: 25 A, T_{on}: 115 μs and T_{off}: 60 μs.
- From the TOPSIS approach, the optimum values of WEDM parameters are: I_p: 25 A, T_{on}: 115 μs and T_{off}: 60 μs, which result in higher MRR with lower SR.
- ANOVA result reveals that I_p is the most significant factor for MRR and SR with a contribution of 74.05%, followed by T_{on} with a contribution of 14.48%. T_{off} is a less significant parameter with a contribution of only 7.18%.
- This research work is very useful for the production of Al7075–10-wt.% ZrO_2 particulate composite related to automotive and aerospace components through the WEDM process.

References

1. A. Manna and B. Bhattacharyya, *Int. J. Adv. Manuf. Technol.* **28** (2006) 67.
2. A. Kumar, T. Soota and J. Kumar, *J. Ind. Eng. Int.* **14** (2018) 821.
3. T. Bera and S. K. Acharya, *Iran. J. Sci. Technol. Trans. Mech. Eng.* **43** (2017) 273.
4. P. Raveendran, S. V. Alagarsamy, M. Ravichandran and M. Meignanamoorthy, *Surf. Rev. Lett.* **28** (2021) 2150021.
5. D. Satishkumar, M. Kanthababu, V. Vajjiravelu, R. Anburaj, S. N. Thirumalai and H. Arul, *Int. J. Adv. Manuf. Technol.* **56** (2011) 975.
6. K. Ponappa, K. S. K. Sasikumar, M. Sambathkumar and M. Udhayakumar, *Surf. Rev. Lett.* **26** (2019) 1950071.
7. B. H. Yan, H. C. Tsai, F. Y. Huang and L. C. Lee, *Int. J. Mach. Tools Manuf.* **45** (2005) 251.
8. F. Muller and J. Monaghan, *Int. J. Mach. Tools Manuf.* **40** (2000) 1351.
9. A. Saha and S. C. Monda, *Silicon* **11** (2019) 1313.
10. R. K. Garg, K. K. Singh, S. Anish, S. Sharma Vishal, O. Kuldeep and S. Sharanjit, *Int. J. Adv. Manuf. Technol.* **50** (2010) 611.
11. S. V. Alagarsamy, M. Ravichandran, S. Dinesh Kumar, S. Sakthivelu, M. Meignanamoorthy and C. Chanakyan, *Mater. Today, Proc.* **27** (2020) 853.
12. A. Goswami and J. Kumar, *Eng. Sci. Technol., Int. J.* **17** (2014) 236.
13. J. W. Liu, T. M. Yue and Z. N. Guo, *Mater. Manuf. Process.* **24** (2009) 446.
14. T. B. Rao, *Adv. Manuf.* **4** (2016) 202.
15. S. S. Mahapatra and A. Patnaik, *Int. J. Adv. Manuf. Technol.* **34** (2007) 911.
16. R. Bobbili, V. Madhu and A. K. Gogia, *Eng. Sci. Technol., Int. J.* **18** (2015) 720.
17. S. Ramabalan, H. B. M. Rajan, I. Dinaharan and S. J. Vijay, *Int. J. Mach. Mach. Mater.* **17** (2015) 295.
18. J. Udaya Prakash, S. Jebarose Juliyana, P. Pallavi and T. V. Moorthy, *Mater. Today, Proc.* **5** (2018) 7275.
19. P. Sreeraj, S. Thirumalai Kumaran, S. Suresh Kumar, M. Uthayakumar and M. Pethuraj, *Surf. Rev. Lett.* **28** (2021) 2050034.
20. N. Lenin *et al.*, *Metals* **11** (2021) 1105.
21. A. Kumar *et al.*, *Adv. Compos. Lett.* **29** (2020) 2633366X20963137.
22. A. Baradeswaran and A. Elaya Perumal, *Compos. B, Eng.* **56** (2014) 464.
23. K. V. Shivananda Murthy *et al.*, *Prog. Nat. Sci., Mater. Int.* **27** (2017) 474.
24. I. Maher and A. A. D. Sarhan, *Int. J. Adv. Manuf. Technol.* **76** (2015) 329.

25. S. V. Alagarsamy, P. Raveendran and M. Ravichandran, *Silicon* **13** (2021) 2529.
26. S. V. Alagarsamy and M. Ravichandran, *Mater. Res. Express* **7** (2020) 016557.
27. S. V. Alagarsamy and M. Ravichandran, *Ind. Lubr. Tribol.* **71** (2019) 1064.
28. A. V. S. Ram Prasad, K. Ramji, M. Kolli and G. Vamsi Krishna, *J. Adv. Manuf. Syst.* **18** (2019) 213.
29. A. A. A. Alduroobi, A. M. Ubaid, M. A. Tawfiq and R. R. Elias, *Int. J. Syst. Assur. Eng. Manag.* **11** (2020) 1314.
30. T. B. Rao and A. G. Krishna, *Int. J. Adv. Manuf. Technol.* **73** (2014) 299.